Colloids and Surfaces B: Biointerfaces 70 (2009) 218–225

Contents lists available at ScienceDirect

Colloids and Surfaces B: Biointerfaces

journal homepage: www.elsevier.com/locate/colsurfb

Surface modification of P(EMA-*co*-HEA)/SiO_2 nanohybrids for faster hydroxyapatite deposition in simulated body fluid?

A. Vallés Lluch[a,*], G. Gallego Ferrer[a,b,c], M. Monleón Pradas[a,b,c]

[a] Center for Biomaterials and Tissue Engineering, Universidad Politécnica de Valencia, Cno. de Vera s/n, 46022, Valencia, Spain
[b] Regenerative Medicine Unit, Centro de Investigación Príncipe Felipe, Av. Autopista del Saler 16, 46013 Valencia, Spain
[c] Networking Research Center on Bioengineering, Biomaterials and Nanomedicine, Valencia, Spain

ARTICLE INFO

Article history:
Received 1 October 2008
Received in revised form 17 December 2008
Accepted 17 December 2008
Available online 27 December 2008

Keywords:
Hybrid
Acrylate
Silica
Bioactivity
Hydroxyapatite

ABSTRACT

P(EMA-*co*-HEA)/SiO_2 nanocomposites with 0, 15 and 30 wt% of silica were obtained by copolymerization of ethyl methacrylate, EMA, and hydroxyethyl acrylate, HEA, during the simultaneous acid-catalyzed sol–gel polymerization of tetraethoxysilane, TEOS. A surface modification treatment was applied in order to reduce the induction time for hydroxyapatite (HAp) nucleation, combining a previous NaOH attack to increase the number of surface nucleating sites, and an alternate soaking process in Ca and P solutions to form apatite precursors, prior to the immersion in a simulated body fluid (SBF). The NaOH treatment was not effective by itself in shortening the HAp induction time. It introduced sodium carboxylates in the copolymer but hydrolyzed the silica network excessively, thus reducing the surface nucleating potential of its boundary silanols. Therefore, bioactivity was only due to the surface carboxylate groups of the organic phase. Maybe a controlled dissolution extent of the silica network so as to improve bioactivity could be attained by reducing the duration of the NaOH-treatment. This would be interesting in the hybrid with 30 wt% of silica, because its dense silica network is not able to hydrolyze in SBF without any previous treatment, whereas the silica network in the hybrid with 15 wt% of silica hydrolyzes at the surface promoting the deposition of HAp. The CaP treatment was able to coat the surfaces of the samples with a calcium phosphate layer within minutes. This amorphous calcium phosphate acted as HAp precursor, skipping the induction period in SBF.

1. Introduction

Biomaterials for mineralized tissue repair need to be biocompatible, osteoconductive, ideally osteoinductive, and mechanically compatible with bone or teeth. Since the discovery of 45S5 Bioglass® (24.5 wt% Na_2O–24.5 wt% CaO–45 wt% SiO_2–6 wt% P_2O_5) by Hench in 1971 [1], various kinds of ceramics such as Na_2O–CaO–SiO_2–P_2O_5 glasses, sintered hydroxyapatite and glass-ceramics containing apatite or wollastonite, have been known to bond to living bone [2–6]. Some of them are being clinically used in artificial middle-ear bone implants, artificial vertebrae, intervertebral discs, iliac bones, fillers in bone and maxillofacial defects or to fill the gap around the implants, etc. and have inspired new bioactive materials [1,6–14]. The bone-bonding materials, so-called bioactive, form a layer of a bone-like carbonate-containing hydroxyapatite on their surface when implanted in the body, and bond to the living bone through this apatite layer. This apatite is a low-crystalline calcium-deficient hydroxyapatite (HAp) containing other ions present in the body fluids such as sodium, magnesium, chlorine and carbonate [1,2,6,15,16]. Based on *in vivo* experiments, in 1991 Kokubo [15] concluded that the essential condition for an artificial material to bond to living bone was the *in vivo* formation of a bone-like apatite layer on its surface when implanted in the living body, and suggested that the bioactivity of a given material could be predicted *in vitro* by a simple biomimetic test. This test consisted in the immersion of the samples in an acellular protein-free simulated body fluid (SBF) with ion concentrations, pH and temperature nearly equal to those of the human blood plasma. It has been widely used since then for the study of biomineralization on different types of materials [7,15–21] and the ability of several materials to form apatite on their surfaces has been correlated with their *in vivo* bioactivities [5].

In the past years, most of the studies with bioactive glasses and glass-ceramics were devoted to the understanding of the mechanism of apatite formation and the roles of the glass constituents, and to obtain simpler bioactive compositions based on the initial system Na_2O–CaO–SiO_2–P_2O_5 [7,15,17–19,22–24]. Two important surface chemical changes are involved in the apatite deposition mechanism on bioactive glasses: (1) preferential diffusion-controlled extraction of Na^+ and/or Ca^{2+} ions out of the glass by exchange with

* Corresponding author. Tel.: +34 96 3877000x88936; fax: +34 96 3877276.
E-mail address: avalles@ter.upv.es (A. Vallés Lluch).

0927-7765/$ – see front matter © 2009 Elsevier B.V. All rights reserved.
doi:10.1016/j.colsurfb.2008.12.027

protons from the solution, and (2) hydration and dissolution of the silica network itself, which is slow at physiological pH [25]. The ion-exchange results in a pH increase and an increase of the ionic activity product (IP) of the HAp in the SBF, which is already saturated with respect to HAp. Hydrolysis of the silica network leads to the release of soluble $Si(OH)_4$ into the medium and formation of °Si–OH groups at the glass-solution interface. These °Si–OH groups provide favourable sites for nucleation of the apatite, while the increasing number of Ca^{2+} ions accelerates the apatite precipitation. The pH of the SBF (7.4) is much greater than the isoelectric point of silica (approximately 2). It is not totally clear yet, but the formed Si–OH groups reveal negative charge that seemingly enhance electrostatic interaction with the positively charged calcium ions in the fluid, resulting in the formation of an amorphous calcium silicate [21,22,26]. The surface thereby acquires a positive charge by accumulation of calcium ions, and interacts electrostatically with the negatively charged phosphate ions in the SBF, leading to the formation of an amorphous calcium phosphate. Once the precursors of apatite or apatite nuclei are formed, they can grow spontaneously by consuming the calcium and phosphate ions from the surrounding body fluid, because the body fluid is already supersaturated with respect to HAp. During this process, the amorphous calcium phosphate incorporates OH^- and $CO_3{}^{2-}$, Na^+, K^+ and Mg^{2+} ions from the solution and finally crystallizes into HAp, which is the most stable calcium phosphate in aqueous media, rendering a porous layer of polycrystalline structures of carbonated-HAp nano-crystals on the surface of the substrate [19,22,23,27].

In fact, calcium ions do not take part in the apatite nucleation itself, but their presence in the silica network facilitates the hydrolysis, and their release to the medium modifies the saturation of the SBF solution. Therefore, the subsequent idea was that bioactivity could be achieved by the formation of specific surface functional groups acting as effective sites for heterogeneous nucleation of apatite, even with Ca and P absent from the composition. In the last years, different functional groups able to develop negative charge at the blood plasma pH, aside from Si–OH, have been found to be effective for calcium phosphate nucleation, *e.g.* phosphate, carboxyl, hydroxyl and amine groups [19-21,23,28,29]. The mechanism of apatite formation is believed to involve electrostatic interactions between the functional groups and the ions from the SBF.

In this context, a wide variety of procedures have been proposed with the aim of improving the bone-bonding ability of bioinert substrates, or of shortening the induction period required for apatite deposition from SBF. These procedures are based on: (a) the pre-calcification of the surfaces, (b) the impregnation of the surfaces with alternative nucleating agents, or (c) the modification of the surfaces with a functional group effective for the apatite nucleation to confer them bioactivity.

Inspired in the previous studies performed on $CaO–SiO_2$-based glasses, Abe et al. [30] developed a biomimetic process to precipitate a HAp layer on bioinert organic polymers, ceramics and metallic materials. Apatite nucleation is carried out by immersing the samples in SBF in the presence of a plate of $CaO–SiO_2$-based glass as a source of nucleating ions of apatite. Silicate ions dissolved from the glass are adsorbed on the substrate to induce apatite nucleation, and dissolution of calcium ions increases the ionic activity product of the apatite in the SBF and accelerates apatite nucleation. Once nucleation occurs, *i.e.*, the surface is pre-calcified, the glass is not needed and apatite nuclei grow on the substrate to form an apatite layer by consuming calcium and phosphate ions from the SBF. Kim et al. [31] and Tanahashi et al. [32] performed similar experiments on polymeric substrates with different sources of nucleating agents. The latter observed that the adhesive strength of the apatite layer to the substrate varied largely with the kind of polymers. It increased with the surface roughness and with the presence of polar groups on the surface, forming a strong bond with the hydroxyl group or calcium ion of the apatite, whereas non-polar polymers bonded to the apatite only by weak van der Waals forces.

Oliveira et al. [28,33] proposed a methodology to generate HAp nucleating sites on the surface of starch-based biodegradable materials or other polymeric biomaterials (with relatively strong swelling ability) and scaffolds, based on the impregnation of the samples with a sodium silicate gel ($Na_2SiO_3H_2O$) containing NaOH. The hydrogen bonding complexes formed between NaOH and hydroxyl groups increase the surface hydrophilicity (higher amount of polar groups in the surface). The alkali attack contributes to the formation of silanol groups that act as apatite inductors. Besides, the adsorption of Ca^{2+} ions leads to the formation of additional nucleating sites by a chelation effect. Other authors achieved apatite formation on silane-coupled polymers by soaking them in titania [34] or calcium silicate [35,36] solutions and afterwards in SBF.

Various surface modification techniques have been proposed aiming to make polymer surface able of inducing apatite nucleation when immersed in SBF. These methods are based on the introduction of hydrophilic polar groups, such as phosphate, hydroxyl groups, Si–OH or Ti–OH, and carboxyl and carboxylate groups, which have been found to be effective for apatite nucleation, onto the hydrophobic substrates [21,37–41].

Taguchi et al. [42] developed a simple method that combines the modification of the surfaces with functional groups effective for the apatite nucleation, and the rapid pre-calcification. In a first step polyethylene substrates were surface-grafted with hydrophilic poly(acrylic acid) or poly(acryl amide) to introduce carboxyl and amide groups, respectively. Afterwards, the pretreated materials were alternatively soaked in Ca and P solutions (CaP treatment), in order to nucleate precursors of apatite in the previously formed nucleating sites. The treatment consisted in dipping the samples consecutively in an aqueous $CaCl_2$ solution for a pre-determined period of time, in ultra-pure water, in aqueous Na_2HPO_4 solution for another period of time, dipped in ultra-pure water, and finally soaking them in acetone and drying. The rapid Ca adsorption was thought to be the key factor in the coating process during the CaP treatment. More recently, Oyane et al. [43] proposed an analogous procedure. In a first step, a poly(ε-caprolactone) substrate was treated with aqueous NaOH to introduce carboxylate groups onto the surface. Afterwards, the NaOH-treated materials underwent an alternate soaking treatment in $CaCl_2$ and $K_2HPO_4{\cdot}3H_2O$ solutions for three consecutive times.

In our previous work [44], a 70/30 wt% copolymer of poly(ethyl methacrylate-*co*-hydroxyethyl acrylate), P(EMA-*co*-HEA), was polymerized during the simultaneous acid-catalyzed sol–gel polymerization of tetraethoxysilane, TEOS, to obtain P(EMA-*co*-HEA)/SiO_2 nanocomposites with different silica contents (0–30 wt%). The incorporation of the silica network aimed at reinforcing the organic matrix and improving its bioactivity. It was found that both the mechanism and the rate of HAp nucleation depended on the chemical reactions occurring at the nanohybrid surfaces when soaked by body fluids. However, once HAp nuclei formed, they rapidly grew on all materials by consuming the calcium and phosphate ions from the solution, leading to porous HAp layers composed of polycrystalline cauliflowers of intricately intertwined needle-like nanocrystals. The induction time for apatite nucleation on the nanohybrid with 15 wt% of silica was 5 days. The rate of apatite nucleation decreased following the sequence H15 > H00 > H30. In the copolymer without silica, the oxygens of the carboxyl and hydroxyl groups probably interacted electrostatically with Ca^{2+} ions from the SBF to form complexes, which then attracted phosphate ions to form calcium phosphate. The absorption of Ca^{2+} ions could contribute to the formation of additional nucleating sites even in inner strata of the material. In the nanohybrid with 15 wt%, the presence of silica considerably improved its

bioactivity. The dissolution of silica at the surface and release of soluble silicates rendered a reaction zone of a few μm, where calcium and phosphate ions were adsorbed and interacted electrostatically with the polar groups of soluble and hydrated silica to form calcium phosphates. The HAp growth continued at the interface hybrid-solution leading to a strongly adhered HAp layer. On the contrary, the dense silica network of the H30 hybrid hindered the diffusion of Ca^{2+} ions through the hybrid and the hydrolysis of the silica network in the interface, and thus the nucleation of HAp occurred even more slowly than on the silica-free copolymer. In the present study, the method developed by Oyane has been followed with the purpose of (i) increasing the number of surface apatite nucleating sites, which will be interesting especially in nanohybrids with superpercolating concentrations of silica, such as H30, where the more perfectly packed silica network contains fewer HAp nucleating silanol groups, and (ii) reducing the incubation times necessary for apatite coating, which could have an application if a thin apatite coat is sought before implantation of the biomaterial to avoid a long induction time and encapsulation.

2. Materials and methods

2.1. Preparation of samples

Two series of nanocomposites of poly(ethyl methacrylate-*co*-hydroxyethyl acrylate), P(EMA-*co*-HEA), 70/30 wt% with 0, 15 and 30 wt% of silica, SiO_2, were obtained in the form of sheets of 0.8 mm in thickness. The synthesis procedure is described in detail in a previous work [45]. Hereafter the samples will be referred to as Hx, x being the percentage of silica (H00, H15 and H30). The hybrids were swollen in a water + ethanol mixture, cut into disk pieces of 8 mm diameter through which a cotton thread was inserted to suspend them in vials, and dried in a vacuum desiccator at 80 °C.

2.2. NaOH treatment and alternate dipping in calcium ion and phosphate ion solutions (CaP treatment)

The two series of samples of H00, H15 and H30 hybrids were immersed in an aqueous solution of NaOH 5 M at 50 °C for 48 h, following the procedure by Oyane et al. [43]. The specimens, removed from the solution, were washed extensively with ultra-pure water, and dried at room temperature in air for a few minutes. Half of the NaOH-treated specimens were soaked alternately in calcium ion and phosphate ion solutions by the following process (hereafter abbreviated as CaP treatment): the specimens were dipped in 200 mM $CaCl_2{\cdot}6H_20$ (99%, Fluka) aqueous solution for 10 s, dipped in ultra-pure water for 1 s and subsequently dipped in 200 mM $K_2HPO_4{\cdot}3H_2O$ (99%, Aldrich) aqueous solution for 10 s and dipped again in ultra-pure water for 1 s. This alternate dipping in calcium and phosphate ion solutions was performed three consecutive times at room temperature.

2.3. Immersion in SBF

The ability of the hybrids to form apatite on their surfaces was tested *in vitro*, by the same procedure as that followed in [44] for the same but non-treated samples. The NaOH-treated samples and those further subjected to the CaP treatment were immersed in SBF for different times up to 35 days in a simulated body fluid (SBF) solution with ion concentrations, pH and temperature nearly equal to those of the human blood plasma, as reported by Kokubo and co-workers [15,30].

In order to obtain the SBF, two solutions were prepared. Solution 1 consisted in 1.599 g of NaCl (99%, Scharlau), 0.045 g of KCl (99%, Scharlau), 0.110 g of $CaCl_2{\cdot}6H_2O$ (99%, Fluka), and 0.061 g of $MgCl_2{\cdot}6H_2O$ (Fluka) in deionized ultra-pure water (Scharlau) up to 100 ml. Solution 2 was prepared by dissolving 0.032 g of $Na_2SO_4{\cdot}10H_2O$ (Fluka), 0.071 g of $NaHCO_3$ (Fluka), and 0.046 g of $K_2HPO_4{\cdot}3H_2O$ (99%, Aldrich) in water up to 100 ml. Both solutions were buffered at pH 7.4, by adding the necessary amounts of aqueous 1 M tris-hydroxymethyl aminomethane, $(CH_2OH)_3CNH_2$ (Aldrich), and 1 M hydrochloric acid, HCl, (37%, Aldrich). Then, both solutions were mixed to obtain SBF with the corresponding molar ion concentrations: 142 Na^+, 5.0 K^+, 1.5 Mg^{2+}, 2.5 Ca^{2+}, 148.8 Cl^-, 4.2 HCO_3^-, 1.0 HPO_4^{2-}, 0.5 SO_4^{2-} mM.

The disks were vertically suspended by the cotton thread in closed glass vials, filled with SBF. The ratio of geometric surface area of glass to solution volume was 0.12 ml mm^{-2}, slightly higher than that proposed by Kokubo [5]. The SBF solution was not renewed during the first 7 days. Afterwards, the ion concentrations were those of SBF multiplied by 2 and the solution was renewed each 2–3 days, in order to provide more favourable conditions for apatite coating. The 2xSBF solution increases the degree of supersaturation to apatite while maintaining the Ca/P atomic ratio, and thus apatite can grow more rapidly. Samples were withdrawn from the SBF after 7 (SBF7), 14 (SBF14) and 35 (SBF35) days, gently washed with ultra-pure water, room conditioned and finally dried in a vacuum desiccator at 80 °C.

2.4. Surface characterization

Scanning electron microscopy, SEM, images of the surfaces were obtained in a JSM-6300 microscope, with the samples previously sputter-coated with gold, 15 kV of acceleration voltage and 15 mm of distance working.

Quantification of elements was achieved by electron dispersive X-ray spectroscopy, EDS, in the mentioned microscope, with the samples previously sputter-coated with carbon, 10 kV of acceleration voltage and 15 mm of distance working. Silicon was employed as optimization standard.

3. Results

3.1. Surface structural changes of the nanohybrids due to the NaOH treatment

After the treatment in the NaOH solution, the H00 and H15 samples remained optically transparent, but those of H30 whitened. In addition, the H15 and H30 samples swelled and bent. Thus, it was not possible to obtain Fourier transform infrared spectra of these samples.

Fig. 1 displays the SEM images of the NaOH-treated samples. H00 and H35 show uniformly spread small deposits on the surfaces, whereas in H15 they seem to be gathered by zones. After the NaOH treatment, the three EDS spectra show the Na peak, and the Si peak is barely detectable in nearly all the obtained hybrid profiles. Fig. 2 shows, as an example, the EDS spectrum of the H30 sample after the NaOH treatment, compared with the original spectrum of H30, which displays a very pronounced silicon peak. The Na and Si contents before and after the NaOH treatment are summarized in Table 1. Before the NaOH treatment, the silica contents calculated from the Si percentages at the surfaces (neglecting the amount of hydrogen in the copolymer and in the silanol groups and the carbon coating of the samples for the EDS measurements) [44] agree well with the nominal contents. After the NaOH treatment, the Si peak is absent and the Na peak appears. The percentage of Na on the surface decreases in the order: H00 > H30 > H15.

3.2. Characterization of the apatite formed on the NaOH-treated nanohybrids

The SEM images of the NaOH-treated H00, H15 and H30 samples and immersed in SBF for the different periods are also displayed

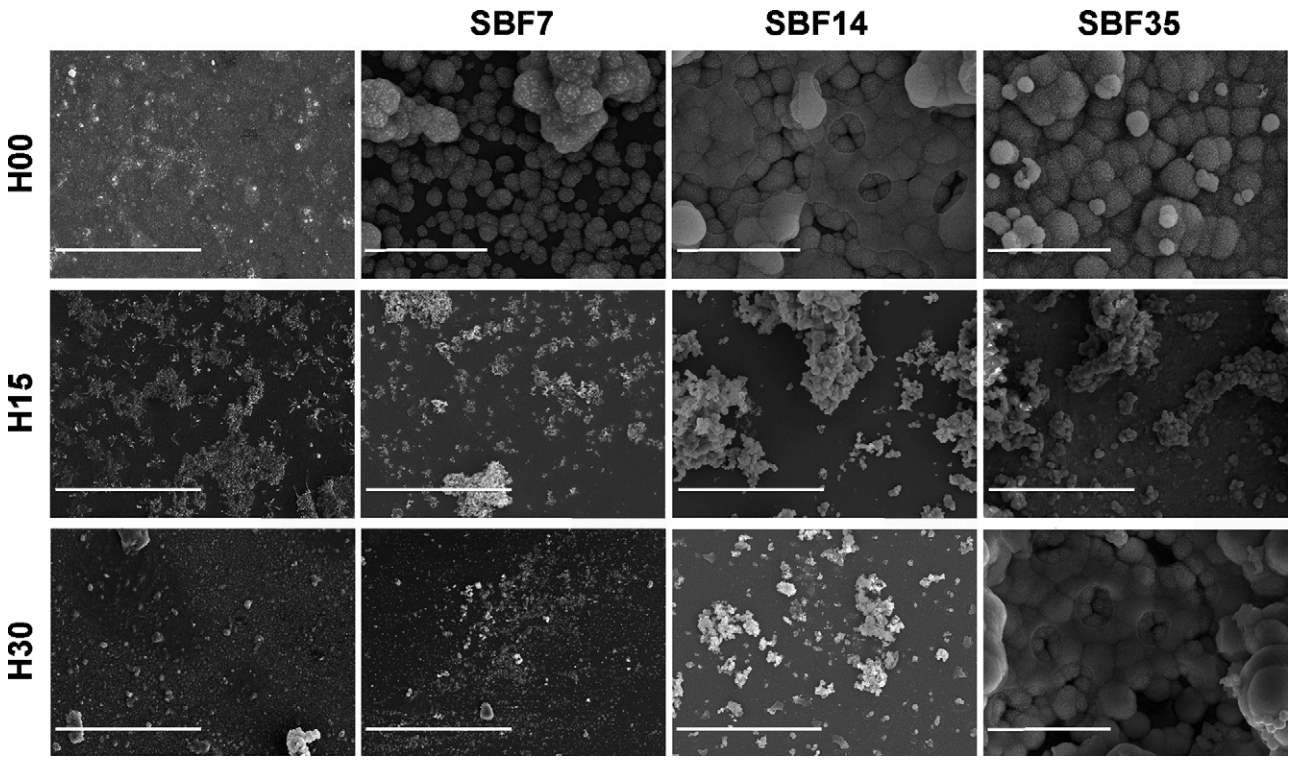

Fig. 1. SEM images of the surfaces of the nanohybrids subjected to the NaOH treatment and subsequently immersed in SBF for different times.

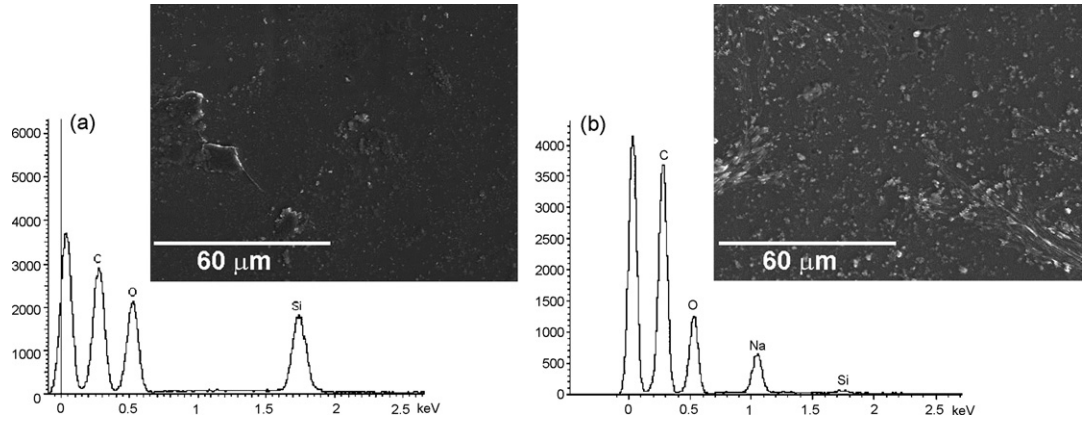

Fig. 2. EDS spectra of H30: (a) before and (b) after the NaOH treatment.

in Fig. 1. After 7 days (SBF7), H00 shows typical intricately intertwined needle-shaped crystals forming some isolated cauliflower HAp structures [5,21,33,34], with an average diameter about 1 μm. After 14 days, more cauliflowers appear on the surface, covered in some zones by continuous semitransparent coatings. With longer times of immersion, the HAp cauliflowers grow in diameter, merge to form a continuous layer, and even exhibit grape-like aggregates of cauliflowers in successive layers leading to very irregular topographies. However, the NaOH-treated H15 and H30 show only scattered deposits within the first 14 days of immersion. At the end of the test, the H15 surface shows the same aspect as H00, whereas the H30 surface presents an aspect similar to H00 after 14 days.

Table 2 summarizes the EDS results of the NaOH-treated samples, after immersion in SBF for different times. The main elements in H00 are Ca and P, but Na, Mg, K and Cl from the SBF also precipitate. The Ca/P atomic ratio presents heterogeneous values. The (Ca + Na + Mg + K)/P is higher than the Ca/P ratio, basically due to the precipitation of NaCl, as reflected by the high Na/Ca and Cl/P ratios,

Table 1
EDS results of the surface of the hybrids initially, after the NaOH treatment and after the CaP treatment (wt% indicates weight percentage, at% indicates atomic percentage).

	non-treated		NaOH-treated			CaP-treated							
	%wt Si	%wt SiO_2	%at Na	%wt Si	%wt SiO_2	%at Ca	%at P	Ca/P	%at Na	%at Cl	%at K	%wt Si	%wt SiO_2
H00	–	–	7.82	–	–	7.32	4.28	1.71	4.71	0.13	0.00	–	–
H15	7.04	15.09	3.94	0.00	0.00	6.75	4.59	1.47	1.66	0.48	1.18	0.22	0.47
H30	13.28	28.45	4.74	0.33	0.71	5.51	3.95	1.39	2.05	0.24	0.86	0.15	0.32

Table 2
Ca/P, (Ca + Na + Mg + K)/P, Na/Ca, Mg/Ca, K/Ca and Cl/P atomic ratios obtained from the EDS results on the hybrids after different times in SBF.

	immersion in SBF																	
	SBF7						SBF14						SBF35					
	$\frac{Ca}{P}$	$\frac{Ca+Na+Mg+K}{P}$	$\frac{Na}{Ca}$	$\frac{Mg}{Ca}$	$\frac{K}{Ca}$	$\frac{Cl}{P}$	$\frac{Ca}{P}$	$\frac{Ca+Na+Mg+K}{P}$	$\frac{Na}{Ca}$	$\frac{Mg}{Ca}$	$\frac{K}{Ca}$	$\frac{Cl}{P}$	$\frac{Ca}{P}$	$\frac{Ca+Na+Mg+K}{P}$	$\frac{Na}{Ca}$	$\frac{Mg}{Ca}$	$\frac{K}{Ca}$	$\frac{Cl}{P}$
H00	1.34	1.85	0.31	0.07	0	0.22	1.38	1.68	0.16	0.04	0.01	0.71	1.48	1.73	0.12	0.04	0	0.09
H15	1.48	1.80	0.11	0.07	0.04	0.26	1.33	1.96	0.34	0.08	0.08	0.37	1.49	1.68	0.07	0.05	0.01	0.08
H30	1.58	1.94	0.06	0.00	0	0.07	1.39	1.60	0.11	0.04	0	0.16	1.65	1.87	0.05	0.04	0.05	0.21
	NaOH treatment + immersion in SBF																	
H00	1.82	2.32	0.33	0.11			1.37	2.62	0.70	0.07	0.07		1.49	3.86	1.48	0.07	0.04	2.70
H15	–						–						1.65	2.29	0.30	0.03	0	0.63
H30	–						–						1.69	3.22	0.91	0.00	0	1.54
	CaP treatment + immersion in SBF																	
H00	1.29	1.85	0.34	0.06	0.03	0.36	1.39	1.97	0.05	0.04	0.33	0	1.53	1.94	0.19	0.04	0.04	0.32
H15	2.00	4.51	1.08	0.13	0.03	1.80	1.34	1.49	0.07	0.04	0	0.04	1.52	2.63	0.68	0.04	0.06	1.53
H30	4.21	15.97	2.30	0.27	0.04	6.19	1.78	13.32	4.51	0.13	0	7.38	2.04	3.14	0.32	0.08	0	0.18

the Mg/Ca and K/Ca ratios being low in all cases. H15 and H30 precipitate salts from the SBF at short times of immersion, basically NaCl. At the end of the test, the Ca/P ratios of the three samples seem to approximate to the physiological ratio (1.65) [31] in the three cases, although the presence of NaCl is still quite relevant.

3.3. Surface structural changes of the nanohybrids due to the CaP treatment

After the CaP treatment, the three types of samples appeared wrinkled and coated with deposits, as can be observed in Fig. 3. Fig. 4 shows the surface of the H00 sample after the CaP treatment at higher magnification. The surface is completely coated and clusters of globular-shaped structures of approximately 100 nm of average diameter are deposited above. The EDS spectra show mainly the Ca and P peaks, but also those from Na, K and Cl. Both K and Cl come from the salts employed in the alternate soaking treatment, while Na is that remaining from the previous treatment. The percentages of Ca and P on the surface decrease in the order: H00 > H15 > H30. Fig. 5 shows the EDS spectrum of the H15 sample initially and after the CaP treatment, as an example. The percentages of the different elements are listed in Table 1.

3.4. Characterization of the apatite formed on the CaP-treated nanohybrids

The SEM images of the CaP-treated samples after the immersion in SBF are shown in Fig. 3. There are not apparently differences between the three types of samples. The soaking in SBF accelerates the deposition of cauliflowers in successive layers, in combination with the deposition of salts. This is evident from the results of the EDS spectra in Table 2. Fig. 6 shows the EDS spectrum of the CaP-treated H00 sample after 14 days in SBF, as an example. The main elements in all cases are Ca and P, but Na, Mg, K and Cl from the SBF also precipitate. The Ca/P atomic ratio presents heterogeneous values and the (Ca + Na + Mg + K)/P is higher than the Ca/P ratio, basically due to the precipitation of NaCl, which is evident from the high Na/Ca and Cl/P ratios. The bottom coatings, *i.e.*, those

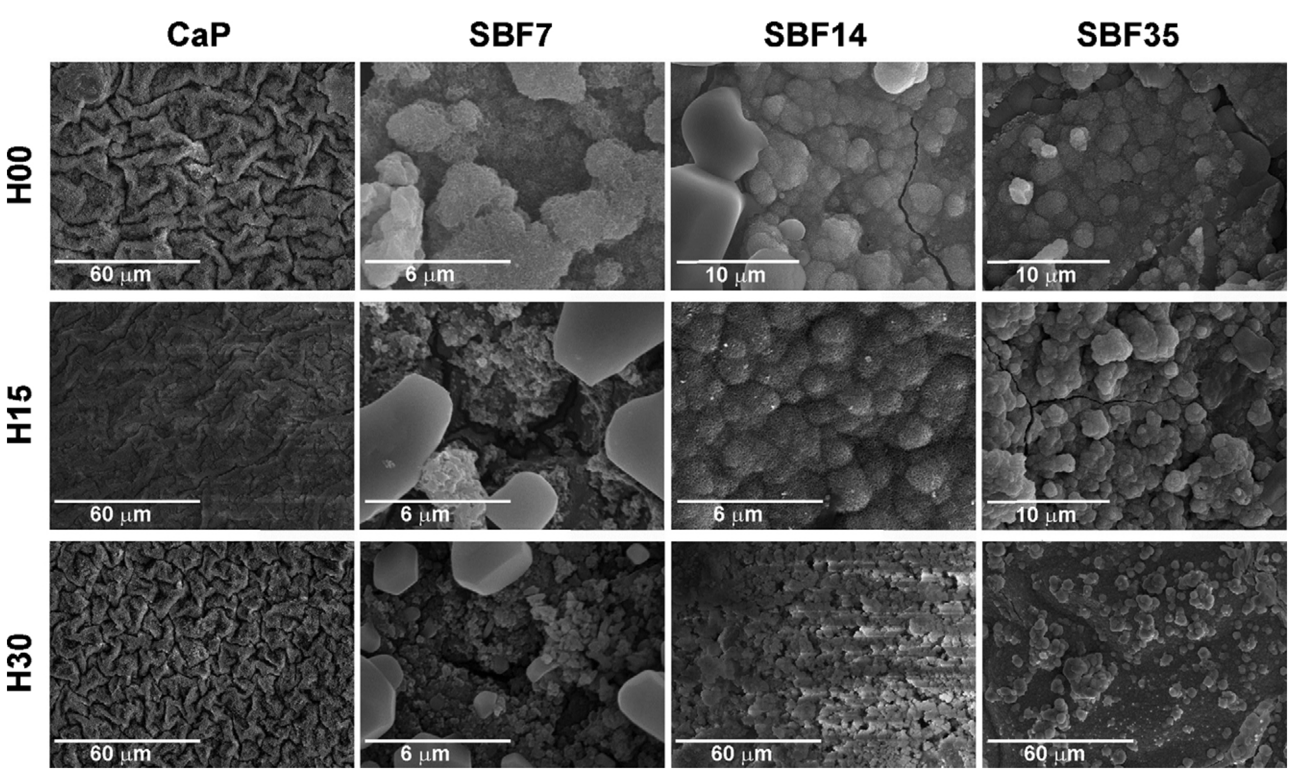

Fig. 3. SEM images of the surfaces of the nanohybrids subjected to the CaP treatment and subsequently immersed in SBF for different times.

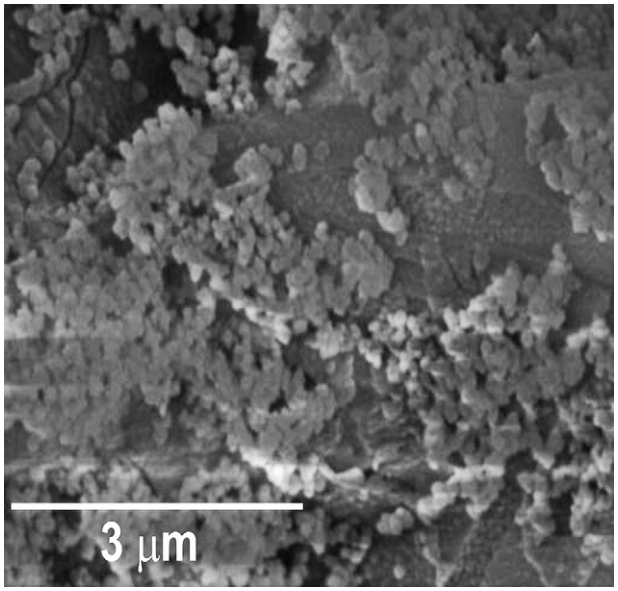

Fig. 4. SEM image of H00 after the CaP treatment.

deposited at short soaking times, are composed of needle-shaped nanocrystals but do not show well defined cauliflowers, nonetheless those formed in 2xSBF do. All the coated surfaces are fairly cracked.

4. Discussion

The presence of the peak ascribed to Na in the EDS spectra after the NaOH treatment, indicates that the surface of the specimens was partially hydrolyzed by the NaOH treatment and the surfaces have been provided with Na-containing groups. The large amount of Na in the copolymer and the practically absence of Si in H15 and H30 indicate that the NaOH treatment notably modifies the copolymer chains at the surface by forming sodium carboxylate in the lateral chains, while it hydrolyzes the silica network, releasing soluble silicates and leaving the surfaces of the hybrids free of silica. Other authors have introduced carboxylate groups in poly(ε-caprolactone) [43] and carboxymethyl chitin [41] by NaOH and $Ca(OH)_2$-treatments, respectively, to confer bone-bonding ability to the former and enhance the catalytic effect of the carboxyl groups in the latter. In our case, the carboxylate formed groups are effective in inducing apatite nucleation with typical needle-like nanocrystals forming globular or cauliflower structures on the copolymer within 7 days, but the scattered cauliflowers formed do not merge to form a continuous layer after more than 14 days. It occurred similarly on the non-treated copolymer (Fig. 7) [44]. The HAp nucleating potential of the non-treated copolymer is due to its lateral carboxyl and hydroxyl groups and its network expansion. The presence of HEA monomer units in the copolymer [44] lowers the glass transition temperature and the modulus of the copolymer with respect to those of PEMA and facilitates the network swelling in an aqueous environment, thereby exposing more efficiently its polar groups. However, PHEA does not nucleate HAp because of its enhanced molecular mobility in comparison with the copolymer, which facilitates the reorganization of its hydroxyl groups and absorption of water more efficiently than they attract Ca^{2+} ions to nucleate HAp.

In the copolymer, the carboxyl and hydroxyl groups probably interact electrostatically with Ca^{2+} ions from the SBF to form complexes, which then attract phosphate ions to form calcium phosphates. On the NaOH-treated copolymer, HAp deposition is initiated by exchange of Na^+ ions with Ca^{2+} ions from the medium, so the formed apatite layer is bonded to the carboxylate groups by ionic interactions [43]. If these hypotheses are true, then it seems reasonable to think that the apatite deposited on the NaOH-treated copolymer will be more strongly anchored to the surface than that grown on non-treated ones.

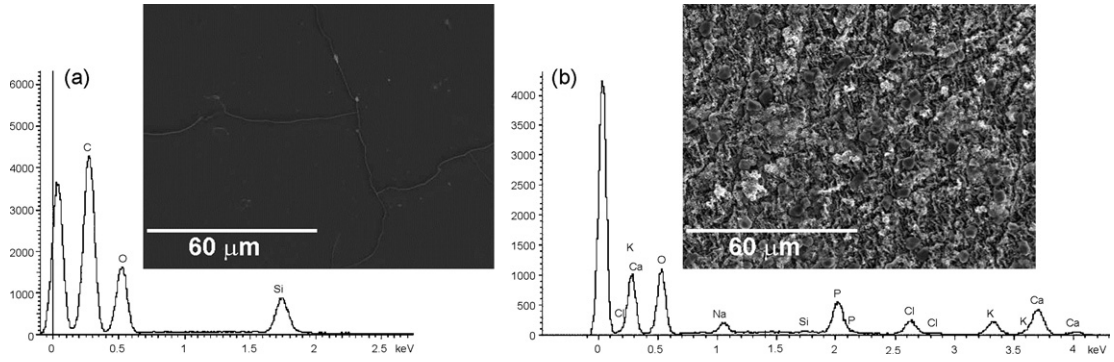

Fig. 5. EDS spectra of H15: (a) initially and (b) after the CaP treatment.

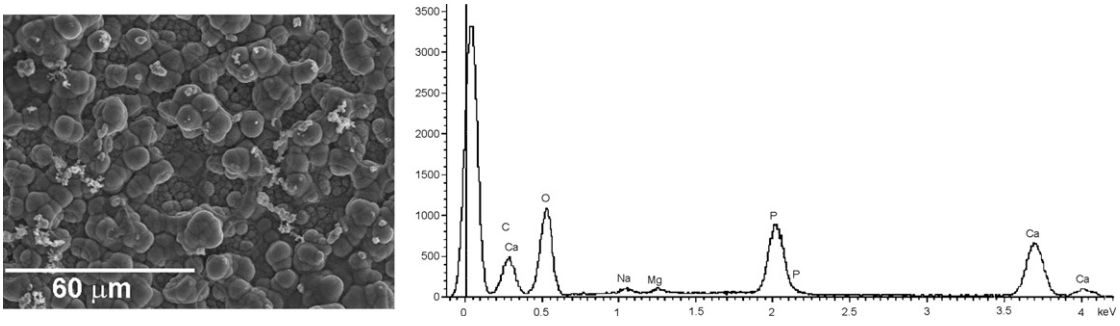

Fig. 6. EDS spectrum of the H00 CaP-treated sample after 14 days in SBF.

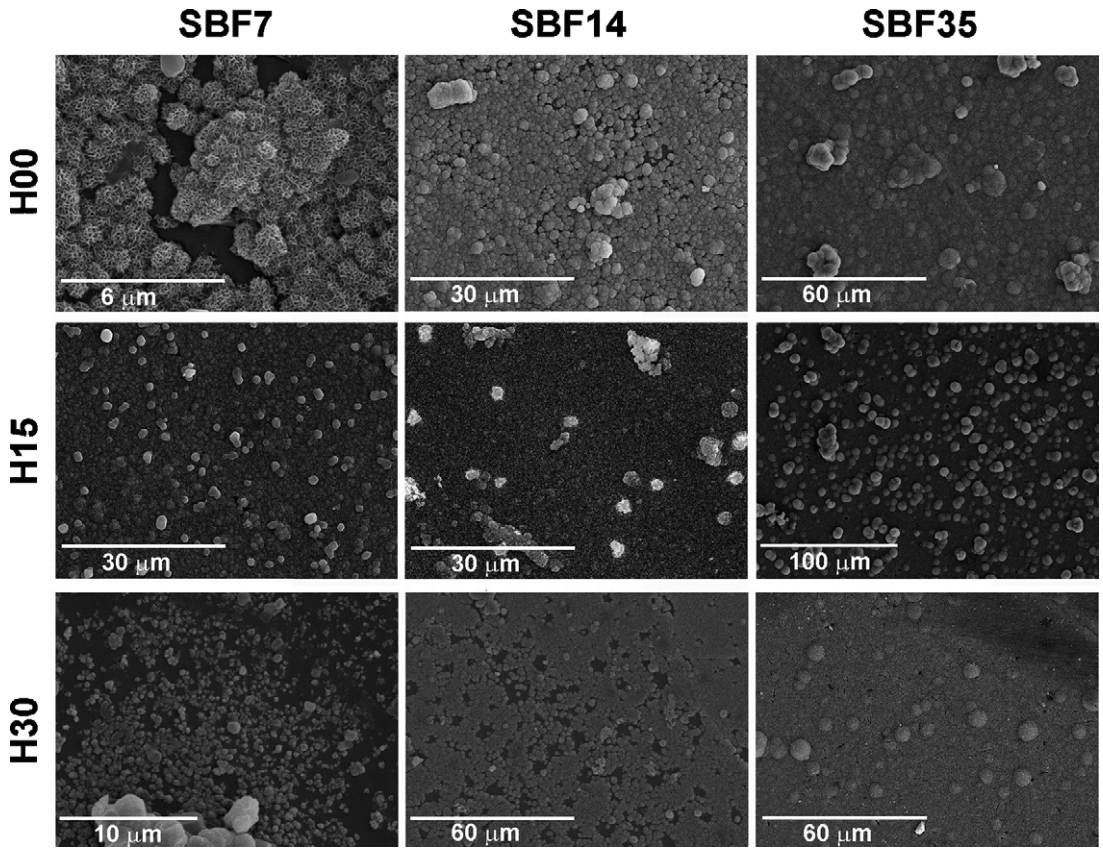

Fig. 7. SEM images of the surfaces of the nanohybrids immersed in SBF for different times.

Besides, the hybrids required longer times to induce the nucleation than the non-treated corresponding samples. On the non-treated nanohybrids (Fig. 7), the heterogeneous nucleation to form the first HAp layer depended on the amount of silica and the nanostructure of the silica network. In H15, the dissolution of silica at the surface was facilitated by the initial relatively high amount of free non-condensed silanol terminal groups in the silica network (due to its discontinuous nature), thereby releasing soluble silicates and rendering an interface layer richer in silanol groups. In this reaction zone of a few μm calcium and phosphate ions were adsorbed and interacted with the polar groups of soluble and hydrated silica to form calcium phosphates. The apatite growth continued at the interface hybrid-solution leading to a strongly adhered apatite layer. After 7 days, the surfaces were completely covered by a HAp layer, and even provided secondary nucleation sites for the deposition of spherical structures with the same needle-like morphology. On the contrary, the densely continuous silica network of H30, with a lower number of free terminal silanol groups, hindered the diffusion of Ca^{2+} ions through the hybrid and the hydrolysis of the silica network at the interface, and thus the nucleation of HAp occurred even more slowly than on the copolymer. In NaOH-treated H15 and H30, silica seems to be absent or at least not available for apatite nucleation, and thus bioactivity is only due to the carboxylate groups of the organic phase. The density and continuity of the silica network hindering the polymer network swelling could be responsible of the longer induction times for HAp nucleation of both nanohybrids with respect to the copolymer. Maybe a suitable dissolution extent of the silica network so as to increase the number of HAp nucleating silanol groups and improve the bioactivity of the original nanohybrid with 30 wt% of silica could be attained by reducing the duration of the NaOH treatment.

The CaP treatment initiates heterogeneous growth of calcium phosphates in SBF instantaneously, as assessed by the SEM images, although the formed apatite cauliflowers within short times in SBF are not well defined and include a large quantity of salts from the SBF. The wrinkled aspect of the samples is probably due to shrinkage. The percentage of calcium phosphate deposited on the surfaces decreases in the order: H00 > H15 > H30, which is in agreement with the order of the amounts of Na deposited in the previous treatment. A longer CaP treatment would probably substitute the remaining Na ions by CaP nuclei. Bioactivity in CaP-treated samples is due only to carboxylate groups, since there are no silanol groups present at the surface. Oyane et al. [43] proposed the following mechanism for the nucleation of calcium phosphate during the alternate soaking process: when the NaOH-treated sample is dipped in the calcium ion solution, the sodium carboxylate groups attract calcium ions from the solution by an ion-exchange reaction. When the specimen is subsequently dipped in the phosphate ion solution, the calcium ions attract negatively charged phosphate ions from the solution. As a result, a certain kind of amorphous calcium phosphate is deposited on the specimen surface with an anchoring effect of the carboxylate groups. These calcium phosphates act as HAp nuclei or precursors of HAp, and spontaneously grow into the HAp layer in SBF, without any induction period, by consuming calcium and phosphate ions from the solution. These amorphous structures provide secondary nucleation sites that nucleate with time HAp cauliflowers of needle-like crystals, with Ca/P ratios approximating to those of physiological (1.65) or stoichiometric (1.67) HAp [31]. This phenomenon of stabilization of amorphous calcium phosphates to poorly-crystalline HAp is well reported in the literature [19,22,23,27], and occurs as well in the NaOH-treated samples at the end of the test. The large amounts of NaCl adsorbed are seemingly due to the high content of NaCl in SBF. The release of Na^+ ions from the samples to the solution could contribute to the deposition of NaCl.

5. Conclusions

The NaOH treatment was not effective by itself in shortening the HAp induction time. It introduces sodium carboxylates in the copolymer lateral chains of the surface and hydrolyzes the silica network, releasing soluble silicates and rendering the surfaces of the hybrids free of silica. Bioactivity is therefore only due to the carboxylate groups of the organic phase. The NaOH-treated and the non-treated copolymer displayed similar apatite nucleation ability, whereas the NaOH-treated hybrids required even longer induction times. Maybe a controlled dissolution extent of the silica network by NaOH (lower duration of the treatment) would improve the low bioactivity of the nanohybrid with 30 wt% of silica.

The posterior CaP treatment is able to coat the surfaces of the samples with a calcium phosphate layer within minutes, the amount of calcium phosphate being dependent of the previous Na deposition. These amorphous or non-apatitic calcium phosphates act as precursors of HAp, and spontaneously grow, without any induction period, by consuming calcium ions and phosphate ions from the solution, as well as a large quantity of salts from the SBF. The initial amorphous structures provide secondary nucleation sites to form successive layers, which stabilize with time rendering HAp layers of polycrystalline cauliflowers with needle-like structure and Ca/P ratios approximating to those of physiological or stoichiometric HAp.

References

[1] L.L. Hench, The story of bioglass, J. Mater. Sci.: Mater. Med. 17 (2006) 967–978.
[2] T. Kokubo, Bioactivity of glasses glass-ceramics, in: P. Ducheyne, T. Kokubo, C.A. Blitterswijk (Eds.), Bone-bonding Biomaterials, Leidendorp: Reed Healthcare Communications, 1992 31-46.
[3] P.K. Bajpai, W.G. Billote, in: J.D. Bronzino (Ed.), The Biomedical Engineering Handbook, CRC Press, University of Iowa, 1995, p. 552.
[4] L.L. Hench, T. Kokubo, in: J. Black, G. Hastings (Eds.), Handbook of Biomaterials Properties, Chapman & Hall, London, 1998 355.
[5] T. Kokubo, H. Takadama, How useful is SBF in predicting in vivo bone bioactivity? Biomaterials 27 (2006) 2907–2915.
[6] B. Ben-Nissan, H.O. Ylänen, Bioactive glasses and glass ceramics, in: M. Akay (Ed.), Wiley Encyclopedia of Biomedical Engineering, John Wiley & Sons, New Jersey, 2006, pp. 354–366.
[7] C. Ohtsuki, T. Kokubo, T. Yamamuro, Mechanism of apatite formation on CaO-SiO_2-P_2O_5 glasses in a simulated body fluid, J. Non-Cryst. Solids 143 (1992) 84–92.
[8] L.L. Hench, Bioceramics, J. Am. Ceram. Soc. 81 (1998) 1705–1727.
[9] K. Zhang, H. Yan, D.C. Bell, A. Stein, L.F. Francis, Effects of materials parameters on mineralization and degradation of sol-gel bioactive glasses with 3D-ordered macroporous structures, J. Biomed. Mater. Res. 66A (2003) 860–869.
[10] M. Kawata, H. Uchida, K. Itatani, I. Okada, S. Koda, M. Aizawa, Development of porous ceramics with well-controlled porosities and pore sizes from apatite fibers and their evaluations, J. Mater. Sci. Mater. Med. 15 (2004) 817–823.
[11] C.Q. Ning, J. Mehta, A. El-Ghannam, Effects of silica on the bioactivity of calcium phosphate composites in vitro, J. Mater. Sci. Mater. Med. 16 (2005) 355–360.
[12] C.C. Ribeiro, C.C. Barrias, M.A. Barbosa, Preparation and characterisation of calcium-phosphate porous microspheres with a uniform size for biomedical applications, J. Mater. Sci.: Mater. Med. 17 (2006) 455–463.
[13] E.S. Thian, J. Hunag, M.E. Vickers, S.M. Best, Z.H. Barber, W. Bonfield, Silicon-substituted hydroxyapatite (SiHA): a novel calcium phosphate coating for biomedical applications, J. Mater. Sci. 41 (2006) 709–717.
[14] J.R. Jones, L.M. Ehrenfried, L.L. Hench, Optimising bioactive glass scaffolds for bone tissue engineering, Biomaterials 27 (2006) 964–973.
[15] T. Kokubo, Bioactive glass ceramics: properties and applications, Biomaterials 12 (1991) 155–163.
[16] T. Kokubo, Design of bioactive bone substitutes based on biomineralization process, Mater. Sci. Eng. C 25 (2005) 97–104.
[17] R. Li, A.E. Clark, L.L. Hench, An investigation of bioactive glass powders by sol-gel processing, J. Appl. Biomat. 2 (1992) 231–239.
[18] A.J. Salinas, M. Vallet-Regi, I. Izquierdo-Barba, Biomimetic apatite deposition on calcium silicate gel glasses, J. Sol-Gel Sci. Tech. 21 (2001) 13–25.
[19] H.M. Kim, T. Himeno, T. Kokubo, T. Nakamura, Process and kinetics of bone-like apatite formation on sintered hydroxyapatite in a simulated body fluid, Biomaterials 26 (2005) 4366–4373.
[20] Zainuddin, D.J.T. Hill, A.K. Whittaker, T.V. Chirila, *In-vitro* study of the spontaneous calcification of PHEMA-based hydrogels in simulated body fluid, J. Mater. Sci.: Mater. Med. 17 (2006) 1245–1254.
[21] T. Kawai, C. Ohtsuki, M. Kamitakahara, K. Hosoya, M. Tanihara, T. Miyazaki, Y. Sakaguchi, S. Konagaya, *In vitro* apatite formation on polyamide containing groups modified with silanol groups, J. Mater. Sci.: Mater. Med. 18 (2007) 1037–1042.
[22] H. Takadama, H.M. Kim, T. Kokubo, T. Nakamura, Mechanism of biomineralization of apatite on a sodium silicate glass: TEM-EDX study in vitro, Chem. Mater. 13 (2001) 1108–1113.
[23] H.M. Kim, T. Himeno, M. Kawashita, T. Kokubo, T. Nakamura, The mechanism of biomineralization of bone-like apatite on synthetic hydroxyapatite: an in vitro assessment, J. R. Soc. Interface 1 (2004) 17–22.
[24] M. Vallet-Regi, A.J. Salinas, D. Arcos, From the bioactive glasses to the star gels, J. Mater. Sci. Mater. Med. 17 (1011) (2006) 1017.
[25] F. Devreux, P. Barboux, M. Filoche, B. Sapoval, A simplified model for glass dissolution in water, J. Mater. Sci. 36 (2001) 1331–1341.
[26] H. Takadama, H.M. Kim, F. Miyaji, T. Kokubo, T. Nakamura, Mechanism of apatite formation induced by silanol groups-TEM observation, J. Ceram. Soc. Japan. 108 (2) (2000) 118–121.
[27] S.A. Hutchens, R.S. Benson, B.R. Evans, H.M. O'Neill, C.J. Rawn, Biomimetic synthesis of calcium-deficient hydroxyapatite in a natural hydrogel, Biomaterials 27 (2006) 4661–4670.
[28] A.L. Oliveira, J.F. Mano, R.L. Reis, Nature-inspired calcium phosphate coatings: present status and novel advances in the science of mimicry, Curr. Opin. Solid State Mater. Sci. 7 (2003) 309–318.
[29] Zainuddin, D.J.T. Hill, A.K. Whittaker, L. Lambert, T.V. Chirila, Preferential interactions of calcium ions in poly(2-hydroxyethyl metyhacrylate) hydrogels, J. Mater. Sci.: Mater. Med. 18 (2007) 1141–1149.
[30] Y. Abe, T. Kokubo, T. Yamamuro, Apatite coating on ceramics, metals and polymers utilizing a biological process, J. Mater. Sci. Mater. Med. 1 (1990) 233–238.
[31] H.M. Kim, K. Kishimoto, F. Miyaji, T. Kokubo, T. Yao, Y. Suetsugu, J. Tanaka, T. Nakamura, Composition and structure of the apatite formed on PET substrates in SBF modified with various ionic activity products, J. Biomed. Mater. Res. 46 (1999) 228–235.
[32] M. Tanahashi, T. Yao, T. Kokubo, M. Minoda, T. Miyamoto, T. Nakamura, T. Yamamuro, Apatite coating on organic polymers by a biomimetic process, J. Am. Ceram. Soc. 77 (1994) 2805–2808.
[33] A.L. Oliveira, P.B. Malafaya, R.L. Reis, Sodium silicate gel as a precursor for the in Vitro nucleation and growth of a bone-like apatite coating in compact and porous polymeric structures, Biomaterials 24 (2003) 2575–2584.
[34] F. Balas, M. Kawashita, T. Nakamura, T. Kokubo, Formation of bone-like apatite on organic polymers treated with a silane-coupling agent and a titania solution, Biomaterials 27 (2006) 1704–1710.
[35] A. Oyane, M. Kawashita, T. Kokubo, M. Minoda, T. Miyamoto, T. Nakamura, Bonelike apatite formation on ethylene–vinyl alcohol copolymer modified with a silane coupling agent and titania solution, J. Ceram. Soc. Japan 110 (2002) 248–254.
[36] A. Oyane, M. Kawashita, K. Nakanishi, T. Kokubo, M. Minoda, T. Miyamoto, T. Nakamura, Bonelike apatite formation on ethylene–vinyl alcohol copolymer modified with silane coupling agent and calcium silicate solutions, Biomaterials 24 (2003) 1729–1735.
[37] M. Tanahashi, T. Yao, T. Kokubo, M. Minoda, T. Miyamoto, T. Nakamura, T. Yamamuro, Apatite coated on organic polymers by biomimetic process: improvement in its adhesion to substrates by NaOH treatment, J. Appl. Biomater. 5 (1994) 339–347.
[38] M. Tanahashi, T. Yao, T. Kokubo, M. Minoda, T. Miyamoto, T. Nakamura, T. Yamamuro, Apatite coated on organic polymers by biomimetic process: improvement in its adhesion to substrate by glow-discharge treatment, J. Biomed. Mater. Res. 29 (1995) 349–357.
[39] K. Kato, Y. Eika, Y. Ikada, Deposition of a hydroxyapatite thin layer onto a polymer surface carrying grafted phosphate polymer chains, J. Biomed. Mater. Res. 32 (1996) 687–691.
[40] A. Oyane, M. Minoda, T. Miyamoto, R. Takahashi, K. Nakanishi, H.M. Kim, T. Kokubo, T. Nakamura, Apatite formation on ethylene–vinyl alcohol copolymer modified with silanol groups, J. Biomed. Mater. Res. 47 (1999) 367–373.
[41] A.M. Kawashita, M. Nakao, M. Minoda, H.M. Kim, T. Beppu, T. Miyamoto, T. Kokubo, T. Nakamura, Apatite-forming ability of carboxyl group-containing polymer gels in a simulated body fluid, Biomaterials 24 (2003) 2477–2484.
[42] T. Taguchi, Y. Muraoka, H. Matsuyama, A. Kishida, M. Akashi, Apatite coating on hydrophilic polymer-grafted poly(ethylene) films using an alternate soaking process.
[43] A. Oyane, M. Uchida, C. Choong, J. Triffitt, J. Jones, A. Ito, Simple surface modification of poly(ε-caprolactone) for apatite deposition from simulated body fluid, Biomaterials 26 (2005) 2407–2413.
[44] A. Vallés Lluch, G. Gallego Ferrer, M. Monleón Pradas, Biomimetic apatite coating on P(EMA-*co*-HEA)/SiO_2 hybrid nanocomposites. Polymer, in review, ref: POLYMER-08-2595.
[45] A. Vallés Lluch, G. Gallego Ferrer, M. Monleón Pradas, Bioactive scaffolds mimicking natural dentin structure, J. Biomed. Mater. Res. Part B: Appl Biomater, in press, doi:10.1002/jbm.b.31272.